

# Magnetic structure and giant magnetoresistance in granular metals

D. Kechrakos<sup>a)</sup> and K. N. Trohidou

*Institute of Materials Science, NCSR "Demokritos," 15310 Athens, Greece*

The effect of dipolar interactions on the giant magnetoresistance (GMR) of a granular metal is studied numerically. The equilibrium magnetic configuration of the system is obtained by classical Monte Carlo simulation and the conductance is calculated using the real space Kubo–Greenwood formula and a single band tight-binding Hamiltonian. The numerical results are compared with experimental finding. © 2000 American Institute of Physics. [S0021-8979(00)72108-6]

## INTRODUCTION

Following the first observation<sup>1</sup> of the giant magnetoresistance (GMR) effect in granular films composed of nano-sized superparamagnetic clusters embedded in a nonmagnetic matrix, a great deal of research effort has been devoted to the understanding of the microscopic mechanism causing the effect and the factors determining its size. As in the case of magnetic multilayers, where GMR was first observed, the effect is attributed to spin dependent scattering of the conduction electrons off the magnetic grains.<sup>2</sup> The value of the GMR in a granular magnetic material depends on the average size of the magnetic grains<sup>1</sup> and the metal volume fraction of the sample.<sup>3,4</sup> Theoretical works on the GMR effect in granular metals include phenomenological models in which the magnetoresistance (MR) is assumed proportional to the moment–moment correlation functions<sup>5–7</sup> and transport treatments using either the classical Boltzmann equation<sup>8,9</sup> or the quantum mechanical Kubo–Greenwood formula.<sup>10,11</sup>

Early experimental studies have demonstrated that the MR follows a quadratic dependence on the reduced magnetization ( $M/M_s$ ) of the sample.<sup>1</sup> This behavior can be understood<sup>5,8</sup> by means of a model of noninteracting superparamagnetic particles with identical magnetic moments. However, deviations from this parabolic relation have been observed by several experimental groups<sup>1,12,13</sup> and were attributed either to grain size distribution<sup>1,12</sup> or to magnetostatic interactions between the grains.<sup>13</sup>

Particle size distribution is mainly responsible for the deviations from the parabola at high fields<sup>1</sup> ( $M/M_s \sim 1$ ) and has been accounted for in previous theoretical models.<sup>6,8</sup> It has also been argued<sup>12</sup> that size distribution effects also contribute to the low field ( $M/M_s \sim 0$ ) deviations, but in this regime it is the interparticle interactions that play the dominant role.<sup>13</sup> This is because interparticle magnetostatic interactions generate short range magnetic order at zero field and consequently the difference in resistance between the saturated and the zero-field state is reduced.

The experimentally observed flattening of the MR vs  $M/M_s$  parabola at low fields has been reproduced within phenomenological models<sup>6,7,12</sup> at the cost of introducing a fitting parameter related to the electronic mean free path with no clear microscopic meaning. More recently, short-range

moment–moment correlations have been included in a semi-classical transport formulation of the MR.<sup>9</sup> However, this model is limited to low concentrations and its application to dense systems is debatable. Also, an explicit form of the short-range moment correlation function that appears in the formalism is not given. A combined study of the micromagnetic structure and the transport coefficients in a granular magnetic metal has not appeared so far.

In this article we obtain the magnetic configuration of a granular metal solid using the Monte Carlo simulation method<sup>14</sup> and we calculate the conductance of the sample using the Kubo–Greenwood expression in the real space representation.<sup>10</sup> Our approach combines the advantage of the phenomenological models,<sup>5–7</sup> namely the realistic description of the micromagnetic configuration of the system with the fully quantum mechanical treatment of the electronic transport that is valid in the whole concentration range and for all values of the scattering potential strength. Particle size effects are not considered here as recent experimental techniques<sup>3,15</sup> have succeeded in growing practically monodisperse samples.

## THE MODEL

We consider identical spherical magnetic grains which we model by an assembly of three dimensional classical spins (magnetic moments) located at random on the sites of a simple cubic lattice. The spins interact via dipolar magnetostatic forces. The total energy of the system reads

$$E = \sum_i \left[ g \sum_j \frac{\hat{m}_i \cdot \hat{m}_j - 3(\hat{m}_i \cdot \hat{R}_{ij})(\hat{m}_j \cdot \hat{R}_{ij})}{R_{ij}^3} - h(\hat{m}_i \cdot \hat{H}) \right], \quad (1)$$

where  $m_i$  is the magnetic moment (spin) of  $i$ th grain,  $g$  is the dipolar strength,  $h$  is the Zeeman energy, and  $R_{ij}$  is the intergranular distance. Hats indicate unit vectors. The energy parameters in Eq. (1) are measured in arbitrary units, while distances are measured in units of the particle diameter. In a previous study<sup>14</sup> we have shown that for temperatures above the blocking temperature of the isolated particles and for a wide range of particle concentrations (up to  $\sim 0.8$ ) the interparticle dipolar interactions have a ferromagnetic character. In this regime, the single-particle anisotropy is immaterial to a first approximation and we therefore do not include the corresponding terms in Eq. (1). A finite sample ( $6 \times 6 \times 6$ , approximately 20 up to 216 spins) is considered with peri-

<sup>a)</sup>Electronic mail: dkehrakos@ims.demokritos.gr

odic boundary conditions. The long range part of the dipolar field is calculated using the Ewald method. The equilibrium spin configuration is obtained by a Monte Carlo simulation using the standard Metropolis algorithm.

To calculate the conductance we consider an electrode-sample-electrode geometry and use a simplified tight-binding Hamiltonian<sup>10</sup>

$$H = \sum_{i,\alpha} \epsilon_i c_{i\alpha}^+ c_{i\alpha} + V \sum_{\langle i,j \rangle, \alpha} c_{i\alpha}^+ c_{j\alpha} - J \sum_{i \in \text{MG}} \sum_{\alpha, \beta} c_{i\alpha}^+ (\hat{m}_i \cdot \hat{\sigma})_{\alpha\beta} c_{i\beta}, \quad (2)$$

where the on-site atomic potentials  $\epsilon_i$  assume the values  $\epsilon_{\text{LW}}$  in the electrodes,  $\epsilon_{\text{NM}}$  in the nonmagnetic matrix and  $\epsilon_{\text{MG}}$  on the magnetic grains. Also,  $V$  is the nearest neighbor hopping integral,  $J$  is the exchange potential of the magnetic material,  $\sigma_x, \sigma_y, \sigma_z$  are the Pauli matrices, and  $\alpha, \beta$  the spin indices. The energy parameters in Eq. (2) are measured in units of the hopping integral ( $V=1$ ). The use of a single-site potential to describe the magnetic grain is justified as long as the electronic mean free path is larger than the particle diameter.

The zero-temperature conductance of the system is given by

$$\Gamma = \frac{2e^2}{h} \text{Tr}(p_z \text{Im}G^{(+)} p_z \text{Im}G^{(+)}), \quad (3)$$

where  $G^{(\pm)} = (E_F - H \pm i\eta)^{-1}$  is the Green function at the Fermi level and  $p_z$  is the component of the electron momentum operator along the axis of current flow ( $z$  axis). Finally, the field-dependent magnetoresistance is defined as  $\text{MR}(H) = [R(H)/R_s - 1] \times 100$ , where the field-dependent resistance  $R(H) = 1/\Gamma(H)$  and  $R_s$  is the resistance of a fully saturated sample.

It is clearly seen from Eq. (2) that the configuration of magnetic moments introduces a distribution of local potentials into the sample that determines its resistance. These potentials are distributed randomly in space but their strengths are spatially correlated according to the moment-moment correlation function. The latter is determined on one hand by the competition between the dipolar interaction energy ( $g$ ) and the Zeeman energy ( $h$ ) and on the other hand on the temperature  $t = k_B T$ .

## RESULTS AND DISCUSSION

For the electronic structure parameters we use  $\epsilon_{\text{LW}} = \epsilon_{\text{NM}} = 0$  so that there is no contribution to the resistance of the system from the electrode-sample contact and from the nonmagnetic matrix. Also we choose  $\epsilon_{\text{MG}} = -2$  and  $J = +2.0$ , so that the electrons in the minority spin band are less scattered by the magnetic grains than those in the majority band, when the grains are aligned ferromagnetically.<sup>10</sup> Finally, we have taken the Fermi level at the band center ( $E_F = 0$ ), in order to give the electrons a Fermi wavelength comparable to the intergranular distance. The Monte Carlo simulation was performed at low temperature ( $t/g = 0.01$ ) so that ordering effects due to dipolar interactions are maximized. The applied field is swept from the negative to the positive saturation value.

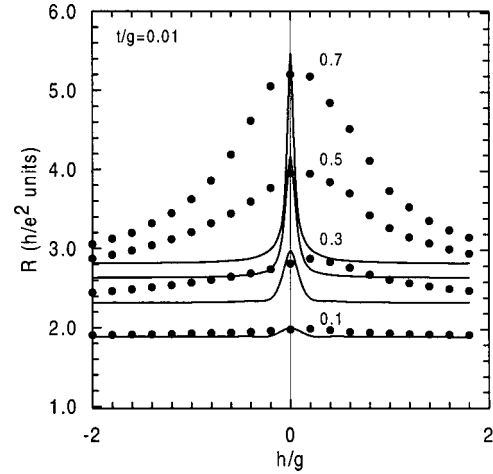


FIG. 1. Resistance as a function of the applied field strength for different particle concentrations. Solid lines: Noninteracting particles. Full circles: Interacting particles.

The field dependence of the resistance and magnetoresistance are shown in Figs. 1 and 2, respectively, for various concentrations of magnetic grains. The characteristic peak close to zero field appears, indicating maximum scattering for the randomly oriented moments. Similar behavior is observed for the dipolar interacting samples, but in this case the curves are modified in three aspects: (a) The maximum values of  $R$  and  $\text{MR}$  are reduced, (b) the saturation field increases with grain concentration, as a result of the competition between the dipolar and Zeeman energies of the dipoles, and (c) a shift of the peak followed by an asymmetry in the shape of the curves appears. In particular, the peak in  $R$  and  $\text{MR}$  shifts to positive fields. This happens because dipolar interactions have an anisotropic character that gives rise to hysteresis. Consequently, the system has a coercive field  $h_c$  and it is around that field that the maximum of the resistance occurs, in agreement with previous numerical<sup>6,7</sup> and experimental<sup>1</sup> studies. Furthermore, the coercive field  $h_c$  is maximum around the percolation limit<sup>14</sup> ( $c_p \sim 0.3$  in our sys-

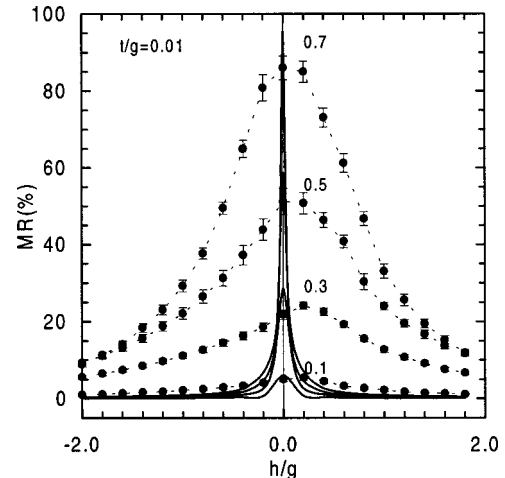


FIG. 2. MR as a function of the applied field strength for different particle concentrations. Solid lines: Noninteracting particles. Full circles: Interacting particles. The dotted line is a guide to the eye.

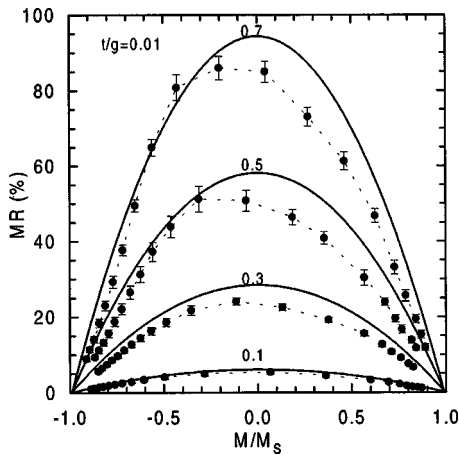


FIG. 3. MR as a function of the reduced sample magnetization for different particle concentrations. Solid lines: Noninteracting particles. Full circles: Interacting particles. The dotted line is a guide to the eye.

tem) and in Figs. 1 and 2 we show that in this concentration range the maximum shift of the resistance peak is observed ( $h_o/g \sim 0.2$  at  $c_p \sim 0.3$ ).

In Fig. 3 we plot the MR data versus the reduced magnetization of the sample for various concentrations. The well known parabolic dependence is reproduced for the noninteracting assembly, while dipolar interactions flatten down the MR vs  $(M/M_s)$  curves at low fields in qualitative agreement with experiments.<sup>13</sup> However, more severe deviations have been measured around the center of the parabola ( $\sim 50\%$  reduction),<sup>12</sup> probably due to the combined effect of the dipolar interactions and the size distribution. The asymmetry of the curves around the maximum value, seen in Fig. 3 for the dipolar systems, is in accordance with the asymmetry of the magnetization curve ( $M-H$  curve) around the coercive field, which reflects the fact that above and below the coercive field the granular system has different micromagnetic configurations.

In Fig. 4 we show the maximum values of the resistance and magnetoresistance as a function of the particle concentration. For weak scattering potentials and dilute systems the resistance increases proportional to the concentration of scatterers.<sup>8</sup> The scattering potential in our model is weak because  $\epsilon_{NM} - \epsilon_{MG} \ll W_B$  and  $J \ll W_B$ , where  $W_B$  is the bandwidth. The linear increase of the resistance for concentrations below the percolation limit, is demonstrated in Fig. 4. This behavior is realized in most granular metals.<sup>2</sup> Deviations from linearity occur in our model above the percolation limit as multiple scattering events become increasingly important.

The MR on the other hand exhibits an almost concave parabolic dependence on the concentration. In a recent theoretical work,<sup>9</sup> it was shown that the concave shape of the concentrational dependence of the MR is an indication of important background spin-independent scattering in the

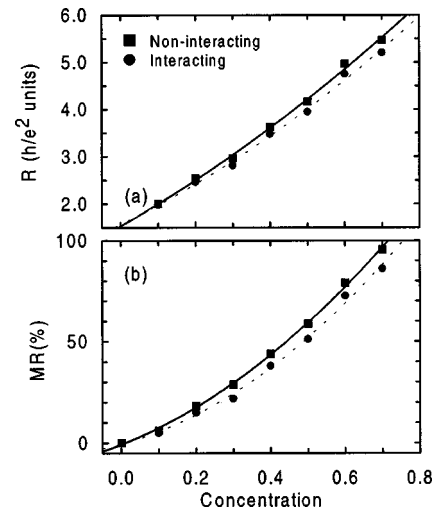


FIG. 4. Dependence of maximum (a) resistance and (b) MR on the concentration of particles. Squares: Noninteracting, Circles: Interacting particles. The lines are guides to the eye.

sample. In our model this is probably the scattering of the electrons at the free boundaries of the sample.

Comparing the magnetoresistance curves in Fig. 4, we notice that the curve of the dipolar system lies below that of the isolated grains. In recent experiments,<sup>3</sup> the concentrational dependence of the MR was fitted to a theoretical model for noninteracting particles<sup>8</sup> and the data fell below the predictions of the model. The discrepancy was attributed to the hypothesis about self-averaging that is inherent in that particular model. Our data in Fig. 4 indicate that dipolar effects could be a candidate for producing the observed discrepancy.

<sup>1</sup>A. E. Berkowitz *et al.*, Phys. Rev. Lett. **68**, 3745 (1992); J. Q. Xiao, J. S. Jiang, and C. L. Chien, *ibid.* **68**, 3749 (1992).

<sup>2</sup>For a review, see, for example, P. M. Levy, Solid State Phys. **47**, 367 (1994).

<sup>3</sup>F. Parent *et al.*, Phys. Rev. B **55**, 3683 (1997).

<sup>4</sup>M. M. Pereira de Alzevedo, G. N. Kakazei, A. F. Kravetz, V. S. Amaral, Yu. G. Pogorelov, and J. B. Sousa, J. Magn. Magn. Mater. **196-197**, 40 (1999).

<sup>5</sup>J. I. Gittleman, Y. Goldstein, and S. Bozowski, Phys. Rev. B **9**, 3609 (1972).

<sup>6</sup>M. El'Hilo, R. W. Chantrell, and K. O'Grady, J. Appl. Phys. **84**, 5114 (1998).

<sup>7</sup>D. Altbir, P. Vargas, J. d'Albuquerque e Castro, and U. Raff, Phys. Rev. B **57**, 13604 (1998).

<sup>8</sup>S. Zhang and P. M. Levy, J. Appl. Phys. **73**, 5315 (1993).

<sup>9</sup>Yu. Pogorelov, M. M. de Azevedo, and J. B. Sousa, Phys. Rev. B **58**, 425 (1998).

<sup>10</sup>Y. Asano, A. Oguri, J. Inoue, and S. Maekawa, Phys. Rev. B **49**, 12831 (1994).

<sup>11</sup>A. Vedyayev, B. Mevel, N. Rhyzhanova, M. Tsiev, B. Dieny, A. Chamberod, and F. Brouers, J. Magn. Magn. Mater. **164**, 91 (1996).

<sup>12</sup>P. Allia, M. Knobel, P. Tiberto, and F. Vinai, Phys. Rev. B **52**, 15398 (1995).

<sup>13</sup>E. F. Ferrari, F. C. S. da Silva, and M. Knobel, Phys. Rev. B **56**, 6086 (1997).

<sup>14</sup>D. Kechrakos and K. N. Trohidou, Phys. Rev. B **58**, 12169 (1998).

<sup>15</sup>S. H. Baker *et al.*, Rev. Sci. Instrum. **68**, 1853 (1997).